Ceacam1L modulates STAT3 signaling to control the proliferation of glioblastoma-initiating cells

Sadahiro Kaneko[1,2], Yuka Nakatani[3,6], Tatsuya Takezaki[3,4], Takuichiro Hide[3,4], Daisuke Yamashita[5], Naoki Ohtsu[1], Takanori Ohnishi[5], Shunsuke Terasaka[2], Kiyohiro Houkin[2], & Toru Kondo[1,3]

[1]Division of Stem Cell Biology, Institute for Genetic Medicine, Hokkaido University, Sapporo, Hokkaido 060-0815, Japan

[2]Department of Neurosurgery, Hokkaido University Graduate School of Medicine, Sapporo, Hokkaido 060-8638, Japan

[3]Laboratory for Cell Lineage Modulation, Center for Developmental Biology, RIKEN, Kobe, Hyogo 650-0047, Japan

[4]Department of Neurosurgery, Kumamoto University Graduate School of Medical Science, Kumamoto, Kumamoto 860-8556, Japan

[5]Department of Neurosurgery, Ehime University Graduate School of Medicine, To-on, Ehime 791-0295, Japan

[6]Present address: Division of Bio-Function Dynamics Imaging, Center for Life Science Technology, RIKEN, Kobe, Hyogo 650-0047, Japan

Correspondence: tkondo@igm.hokudai.ac.jp

Running title: Ceacam1L as a new GIC regulator

Keywords: Glioblastoma (GBM)/GBM-initiating cells (GICs)/Ceacam1L/c-Src/STAT3

Summary

Glioblastoma (GBM)-initiating cells (GICs) are a tumorigenic subpopulation that are resistant to radio/chemotherapies and are the source of recurrence; however, the molecular mechanisms by which GICs are maintained have not yet been elucidated in detail. We herein demonstrated that carcinoembryonic antigen-related cell adhesion molecule 1 with a long-cytoplasmic tail (Ceacam1L), a homo/heterophilic intercellular-binding membrane protein, acted as a crucial factor in GIC maintenance and tumorigenesis through the activation of c-Src/STAT3 signaling. Using a chimeric transmembrane protein with a Ceacam1L-cytoplasmic tail, we further showed that the monomeric Ceacam1L-cytoplasmic tail bound with c-Src and STAT3 and induced their phosphorylation, whereas its oligomerization resulted in the loss of this function. Our results suggest that Ceacam1L-dependent intercellular adhesion between GICs and their surrounding cells plays an essential role in GIC maintenance and proliferation through the monomeric Ceacam1L-cytoplasmic tail.

Introduction

Gliomas are brain tumors possessing the characteristics of glial cells, astrocytes, and oligodendrocytes, and have been classified into four grades (WHO grade I-IV) based on their pathological features. Glioblastoma (GBM) is the most malignant glioma (WHO grade IV), and patients with GBM have a median survival of approximately one year. In spite of tremendous efforts to effectively treat GBM, the overall survival rates of patients with GBM have remained unchanged over the past few decades.

The discovery of GBM-initiating cells (GICs) has had a significant impact on GBM research (1). GICs have been shown to self-renew indefinitely, express stem cell markers, such as CD133 (also known as Prominin1), CD15 (also known as Stage-Specific Embryonic Antigen 1 and Lewis X) and CD49f (also known as integrin α6), and be more resistant to radio- and chemo-therapies than non-GICs (2-4). GICs are likely to exploit the signaling pathways involved in maintaining NSCs (2-4). NSCs only exist in the subventricular zone and hippocampus (5,6), both of which contain a special microenvironment (niche) for the maintenance of NSCs, whereas GBM arises in many areas in the brain. It currently remains unknown whether GICs generate a NSC niche anywhere or employ an unknown mechanism for their maintenance in non-NSC niches.

We previously established the mouse GIC (mGIC) lines, NSCL61 and OPCL61, by overexpressing an oncogenic $HRas^{L61}$ in *p53*-deficient NSCs and oligodendrocyte precursor cells (OPCs), respectively (7,8). These mGICs formed transplantable GBM with hypercellularity, pleomorphism, multinuclear giant cells, mitosis, and necrosis, even when as few as ten cells were injected into the brains of nude mice. These findings indicated that

they were highly enriched in GICs. Using DNA microarray analyses, we compared the gene expression profiles of mGICs with those of their parental cells and identified genes that were up-regulated and down-regulated in mGICs. By evaluating the candidate genes using human GIC (hGIC) lines and GBM tissues, we successfully selected potential GIC-specific genes (7-9).

Among the candidate genes evaluated, we focused on Carcinoembryonic antigen-related cell adhesion molecule 1 (Ceacam1, also known as CD66a and BGP1). Human Ceacam1 consists of 11 splicing variants, seven of which are transmembrane proteins with either a short (Ceacam1S) or long cytoplasmic tail (Ceacam1L) while the others are secretion forms (10-12). Transmembrane Ceacam1 exists as a monomer, cis-/trans-homodimer, or cis-/trans-heterodimer with either Ceacam1 splicing variants or other Ceacam family members depending on the cell environment; therefore, the intracellular domain of Ceacam1 is a monomer or a homo-/hetero-dimer (11,12), which transmit different signals. Ceacam1 was previously shown to be involved in many different biological functions, including angiogenesis, insulin clearance, immune modulation, and proliferation (10-12). Ceacam1L was also identified as a substrate of the insulin growth factor receptor and epidermal growth factor receptor (EGFR), both of which are frequently activated in malignant gliomas (13), while modified Ceacam1 acted as either an amplifier or attenuator of these receptors in a cell-dependent manner. These findings prompted us to investigate the role of Ceacam1 in GICs.

Materials and Methods

Animals and Chemicals

Animals were obtained from the Laboratory for Animal Resources and Genetic Engineering at the RIKEN Center for Developmental Biology (CDB) and from Charles River Japan, Inc. All mouse experiments were performed following protocols approved by the Animal Care and Use Committees of RIKEN CDB, Ehime University, and Hokkaido University. Chemicals and growth factors were purchased from Sigma and PeproTech, respectively, except where indicated.

Cell culture

Mouse primary neural cells (NSCs and OPCs), NSCL61, OPCL61, human NSCs (hNSCs, Invitrogen), and GICs (hGICs, E3 and E6) were cultured as described previously (7-9,14). Cells were cultured in chamber slides (Nunc) precoated with fibronectin and poly-D-lysine for immunostaining, as described previously (14).

Immunochemistry

Immunostaining of paraffin-embedded human brain-tumor sections (6 μm thick) and mouse cells or brain sections was performed as described previously (7,8). Ceacam1 was retrieved by HistoVT One according to the supplier's instructions (Nacalai Tesque). The sections were permeabilized with 0.3% TritonX-100 in PBS for penetration, treated with a blocking solution (2% skim milk, 0.3% Triton X-100, and PBS) for 1 h, and incubated with primary antibodies for 16 h at 4°C. Cells were fixed and immunostained as described previously

(14). The following antibodies were used to detect antigens: mouse anti-Ceacam1 (1:50; R&D), anti-GFAP (1:500; Chemicon, 1:400; Sigma for human cells), rat monoclonal anti-GFP (1:500 ; Nacalai Tesque), mouse monoclonal anti-Nestin (1:200; BD), mouse monoclonal anti-CD15 (1:200; BD Pharmingen), rabbit polyclonal anti-STAT3 (1:100; Santa Cruz), rabbit polyclonal anti-phosphorylated STAT3 (1:100; Cell Signaling Technology), rabbit polyclonal anti-EGFR (1:50; Cell Signaling Technology), rabbit polyclonal anti-Caspase 3 (1:1000, Cell Signaling Technology) and rabbit monoclonal anti-Ki67 (1:200, Thermo Scientific). Antibodies were detected with Alexa568-conjugated goat anti-rabbit IgG (1:500 Molecular Probe), Alexa488-conjugated goat anti-mouse, -rabbit, or -rat IgG (1:500; Molecular Probe) and goat anti-mouse IgG-Cy3 (1:500; Jackson ImmunoResearch). Cells were counterstained with DAPI (1 μg/ml) to visualize the nuclei.

Human brain tumors

hGICs were used according to the research guidelines of the Ehime University Graduate School of Medical Science and the Hokkaido University Institute for Genetic Medicine. The detailed characterization of hGICs has been reported in (9). Poly(A)+ RNA was prepared using a QuickPrep mRNA Purification Kit (GE Healthcare). Control human brain total mRNA (CB) was purchased from Invitrogen. cDNA was synthesized using a Transcription First Strand cDNA Synthesis Kit (Roche).

RT-PCR

RT-PCR was carried out as described previously (14), with the cycle parameters of 20 sec at 94°C, 30 sec at 57°C, and 60 sec at 72°C for 35 cycles (GICs) or 40 cycles (GBM tissues). Cycles for *gapdh* were 15 sec at 94°C, 30 sec at 53°C, and 90 sec at 72°C for 22 cycles. The following oligonucleotide DNA primers were synthesized: for mouse *Ceacam1*, the 5' primer was 5'-ATCCTCCCAAGAGCTCTTTATC-3', and the 3' primer was 5'-TTTGTGCTCTGTGAGATCTCG-3'; for human *Ceacam1*, the 5' primer was 5'-ACACCATGGGGCACCTCTCA-3', and the 3' primer was 5'-GATCGTCTTGACTGTGGTCCT-3'; for *sox1*, the 5' primer was 5'-AGGGCTACATGAGCGCGTCG-3', and the 3' primer was 5'-CTAGATGTGCGTCAGGGGCA-3'; for *aldh1a1*, the 5' primer was 5'-AGGGGCAGCCATTTCTTCTC-3', and the 3' primer was 5'-GGCAATGCGCATCTCATCTG-3'; for *cxcr4*, the 5' primer was 5'-CTGACCTCCTCTTTGTCATCAC-3', and the 3' primer was 5'-GTCTTGAGGGCCTTGCGCTT-3'; for *dll1*, the 5' primer was 5'-TGGTGGTCTGCGTCCGGCTG-3', and the 3' primer was 5'-ACCGACTGGTACTTGGTGTC-3'; for *notch3*, the 5' primer was 5'-ATGGTGGAAGAGCTCATCGC-3', and the 3' primer was 5'-TGGCCTCCTGCTCTTCTTGG-3'; for *hey1*, the 5' primer was 5'-GCGGACGAGAATGGAAACTTG-3', and the 3' primer was 5'-AGTCCTTCAATGATGCTCAGAT-3'; for *egfr*, the 5' primer was 5'-GATGAAAGAATGCATTTGCCAAG-3', and the 3' primer was 5'-GGGGCTGATTGTGATAGACAGG-3'; for *stat3*, the 5' primer was

5'-GTGTCAGATCACATGGGCTAA-3', and the 3' primer was 5'-TGCCTCCTCCTTGGGAATGT-3'; for *ptpn6*, the 5' primer was 5'-GTGTCCTCAGCTTCCTGGAC-3', and the 3' primer was 5'-GTCTGTCCATCGCGAAATGC-3'; for *ptpn11*, the 5' primer was 5'-AAAGGGGAGAGCAATGACGG-3', and the 3' primer was 5'-ATTCACCGTGTTTTGCAGGC-3'; for *c-Src*, the 5' primer was 5'-ACATCCCCAGCAACTACGTG-3', and the 3' primer was 5'-AGCTTCTTCATGACCTGGGC-3'. The primers for *gapdh* were described previously (14).

Flow cytometry

hGICs were immunolabeled with rabbit polyclonal anti-Ceacam1 (5μg/ml; LSBio) and mouse monoclonal anti-CD15 (5μg/ml; BD Pharmingen), following with Alexa 488-conjugated goat anti-mouse IgG (1:400; Molecular Probe) and Cy5-conjugated goat anti-rabbit IgG (Molecular Probe; diluted 1:400). The cells were analyzed in an Aria II (Becton Dickinson) using a dual-wavelength analysis (488 nm solid-state laser and 638 nm semiconductor laser). Propidium iodide (PI)-positive (i.e., dead) cells were excluded from the analysis.

The SP was analyzed as shown previously (15). Reserpine (10 μM), an inhibitor of some ABC transporters, was used to identify SP.

Vector construction

Complementary DNAs (cDNAs) were cloned as described previously (7). Human *ceacam1L* cDNA was inserted into pcDNA3.1-hyg (Invitrogen), pcDNA3-2xFLAG-c and pMY-EGFP vectors to produce pcDNA3.1 -hyg-hCeacam1L, pcDNA3-hCeacam1L-2xFLAG-c and pMY-EGFP-hCeacam1L. The following oligonucleotide DNA primers were synthesized: for the full-length human *ceacam1L*, the 5' primer was 5'-AGCTAGCGCCACCATGGGGCACCTCTCAGCCCC-3', and the 3' primer was 5'-ACTCGAGTTACTGCTTTTTTACTTCTGAATA-3'; for the FLAG-tagged human *ceacam1L*, the 5' primer was 5'-AGAATTCGCCACCATGGGGCACCTCTCAGCCC-3', and the 3' primer was 5'-ACTCGAGCTGCTTTTTTACTTCTGAATAAATTAT-3'. Mouse *ceacam1L* cDNA was also cloned and inserted into the pcDNA3-2xFLAG-c vector to produce pcDNA3-mCeacam1L-2xFLAG-c. The following oligonucleotide DNA primers were synthesized: the 5' primer was 5'-AGAATTCGCCACCATGGAGCTGGCCTCAGCACA-3', and the 3' primer was 5'-ACTCGAGCTTCTTTTTTACTTCTGAATAAAC-3'.

To knockdown human and mouse *ceacam1*, short-hairpin (sh) sequences were generated using InvivoGen's siRNA Wizard (HYPERLINK "http://www.sirnawizard.com/" http://www.sirnawizard.com/). These sh sequences were inserted into a psiRNA-h7SKhygro G1 expression vector (InvivoGen) to produce psiRNA-h7SKhygro-mceacam1sh and psiRNA-h7SKhygro-hceacam1sh. The knockdown efficiency of these vectors was analyzed by Western blotting (Supplemental Figure S3). The sh target sequences for human and mouse *ceacam1* were 5'-ACCTCGGATGGCAACCGTCAAATTGTTCAAGAGACAATTTGACGGTTGCCAT

CCTT-3’ and 5’-ACCTCGGGAAACACTACGGCTATAGATCAAGAGTCTATAGCCGTAGTGTTTCC CTT-3’, respectively. The control sh target (*egfp*) sequence was 5’-GCAAGCTGACCCTGAAGTTCA-3’.

To construct the FGC1L expression vector, we amplified a portion of the mouse GCSFR extracellular domain (AA309-626) from pBOS-I62 (a kind gift from Dr. Shigekazu Nagata of Kyoto University) and the transmembrane domain-cytoplasmic tail of Ceacam1L from pcDNA3.1-hyg-hCeacam1L as described previously (7) . We then inserted these fragments into p3XFLAG-CMV-9 vector (SIGMA) to produce the p3XFLAG-GCSFR-Ceacam1L cytoplasmic tail (pFGC1L). The following oligonucleotide DNA primers were synthesized: for the mouse GCSFR extracellular domain, the 5' primer was 5’-TGCGGCCGCGCGATGCATTCGCTCATCTCTG-3’, and the 3' primer was 5’-AAGATCTCTCGAGTTACTGCTTTTTTACTTCTGAATA-3’; for the transmembrane domain-cytoplasmic tail of Ceacam1L, the 5' primer was 5’-TCCATCTGACATTGTGATTGGAGTAGTGGC-3’, and the 3' primer was 5’-ACTCGAGTTACTGCTTTTTTACTTCTGAATA-3’.

FGC1S was amplified from pFGC1L and inserted into the p3XFLAG-CMV-9 vector to produce the p3XFLAG-GCSFR-Ceacam1S cytoplasmic tail (pFGC1S). The following oligonucleotide DNA primers were synthesized: the 5' primer was 5’-TGCGGCCGCGCGATGCATTCGCTCATCTCTG-3’, and the 3' primer was 5’-AAGATCTCTCGAGTCATTGGAGTGGTCCTGAGCT-3’.

The nucleotide sequences of cloned cDNA were verified using the BigDye Terminator Kit version 3.1 (Applied Biosystems) and ABI sequencer model 3130xl (Applied Biosystems).

We transfected cells with the vectors using either the Nucleofector device according to the supplier's instructions (Lonza) or Polyethylenimine (PEI), as previously described (7,16).

Intracranial cell transplantation into immunodeficient mouse brains

To mark the transplanted hGICs in vivo, the cells were transfected with pMY-EGFP or pMY-EGFP-hCeacam1L vector as described previously (7,8). The GFP-expressing hGICs (hereafter, hGICs) and *ceacam1L*-overexpressing hGICs were suspended in 5 μl of culture medium and injected into the brains of 5~8 week-old female NOD/SCID mice that had been anesthetized with 10% pentobarbital. The stereotactic coordinates of the injection site were 2 mm forward from the lambda, 2 mm lateral from the sagittal suture, and 5 mm deep.

Mouse brains were dissected, fixed in 4% paraformaldehyde overnight, transferred to 70% ethanol, processed on Tissue-Tek VIP (Sakura Finetek Japan, Tokyo, Japan), and embedded in paraffin. Coronal sections (6 μm thick) from the cerebral cortex were prepared on a microtome and stained with hematoxylin-eosin (HE).

Proliferation assay

Two thousand cells were cultured in 100μl of the culture medium in each well of a 96-well plate. To examine cell proliferation, the MTT assay was performed as follows. Ten

microliters of MTT (5mg/ml, Nacalai Tesque, Japan) was added to each well on days 0, 2 or 3, and 4 *in vitro*. The cells were incubated for 4 hr, the medium was replaced with 100μl of DMSO, the cells were dissociated, and cell proliferation was quantified on a Benchmark microplate reader (Bio-Rad) with the absorption spectrum at 570nm.

Soft agar assay

We performed a soft agar assay in order to determine whether transfected cells proliferated in an anchorage-independent manner. The transfected cells were suspended in 0.3% top agar made with the optimized medium and layered onto 0.6% bottom agar made with the same medium. After the top agar had polymerized, culture medium was added and the cells were cultured for 20d with medium changes every three days.

Microarray hybridization and data processing

Total RNA was extracted from mouse NSCs and NSCL61 using the TRIzol Plus RNA Purification System (Invitrogen). Purified RNA was then amplified and labeled with Cyanine 3 (Cy3) using the one-color Agilent Low Input Quick Amp Labeling Kit (Agilent Technologies) following the manufacturer's instructions. Labeled cRNAs were fragmented and hybridized to the Agilent mouse GE 8x60K Microarray. After washing, microarrays were scanned with an Agilent DNA microarray scanner. Intensity values for each scanned feature were quantified using Agilent feature extraction software, which performed background subtractions.

Normalization was achieved using Agilent GeneSpring GX version 11.0.2. After normalization, hierarchical sample clustering of the expressed genes (DEGs) was performed with the Euclidean distance and average linkage methods (Agilent GeneSpring GX).

Accession number for microarray data: http://www.ncbi.nlm.nih.gov/geo/query/acc.cgi?acc=GSE70023

Brain fixation and histopathology

Dissected mouse brains were fixed in 4% paraformaldehyde at 4°C overnight. After fixation, the brains were cryoprotected with 12-18% sucrose in PBS and embedded in Tissue-Tek OCT compound (Miles, Elkhart, IN). Coronal sections (6 μm thick) were prepared from the cerebral cortex and stained with hematoxylin-eosin (H&E) using a standard technique or immunolabeled for GFP and either the active form of Caspase 3 to detect dying cells or Ki67, a marker for proliferating cells.

Immunoprecipitation and Western blotting

Immunoprecipitation was performed as previously described (17). Cell lysates were incubated with Protein G sepharose (GE Healthcare) and the anti-FLAG (10 μ/ml) antibody for 4 h at 4°C. The mixtures were centrifuged, and the precipitants were triple-washed and analyzed by Western blotting.

Western blotting was performed as previously described (17). The blotted membranes were probed with anti-Nestin (1:1000; BD Pharmingen, 1:200; Chemicon for

human cells), anti-GFAP (1:1000; BD Pharmingen, 1:200; Chemicon for human cells), rabbit anti-STAT3 (1:1000; Santa Cruz), rabbit anti-phospho-STAT3 (1:1000; Cell Signaling Technology), rabbit anti-PTPN6 (1:1000; Cell Signaling Technology), rabbit anti-PTPN11 (1:1000; Cell Signaling Technology), rabbit anti-phospho-PTPN11 (1:1000; Cell Signaling Technology), rabbit anti-c-Src (1:1000; Cell Signaling Technology), rabbit anti-phospho-c-Src (1:1000; Cell Signaling Technology), or a mouse anti-GAPDH antibody (1:1000; Chemicon). An ECL system (Amersham) was used for detection.

Statistical analysis

Survival data were analyzed for significance by Kaplan-Meier methods using GraphPad Prism version 4 software (*p-values* were calculated with the Log-rank Test). All experiments were conducted more than three times with similar results.

Results

Ceacam1L was identified as a novel GIC marker

We confirmed that the expression of *ceacam1L* was higher in NSCL61, OPCL61, and hGICs, E3 and E6 that were prepared from human GBM tissues, than in mouse parental cells (*p53* deficient-mNSCs and -mOPCs) or normal human NSCs (hNSCs) (Fig. 1A) (7,9). An immunocytochemical analysis revealed that over 70% of cultured human and mouse GICs were positive for Ceacam1 (Fig. 1B). *Ceacam1L* was more prominently expressed in GBM than in other malignant gliomas, anaplastic astrocytoma (AA), anaplastic oligo-astrocytoma (AOA), or anaplastic oligodendroglioma (AO) (Fig. S1A). Although *ceacam1S* was expressed in mouse and human GICs, the expression level of *ceacam1S* was significantly lower than that of *ceacam1L* in hGICs (Fig. S1B and S1C). Furthermore, over 70% of Ceacam1-positive cells were co-immunolabeled for the well-known GIC marker CD15 in the periphery of human GBM (18) (Fig. 1C), while all Ceacam1^{+} cells were positive for EGFR, which is frequently amplified in human GBM (1,13) (Fig. 1D). Flow cytometric analysis showed that 3.2% of freshly prepared GBM cells were Ceacam1^{high} and over 90% of Ceacam1^{high} cells (2.9% in total) were also positive for CD15 (Fig. 1E). Taken together, these results suggested that Ceacam1 was a novel GIC marker.

Ceacam1L was involved in GIC proliferation and angiogenesis

We analyzed the function of Ceacam1L in GICs. Using *ceacam1L*-specific shRNA (*ceacam1sh*) expression vectors (Fig. S2), we found that the depletion of Ceacam1L inhibited the proliferation of human and mouse GICs (Fig. 2A) as well as their colony

forming ability in soft agar (Fig. 2B). In contrast, *ceacam1L*-overexpressing hGICs enhanced their colony forming activity in soft agar (Fig. 2C) and killed mice more quickly than their parental cells (Fig. 2D). H&E staining revealed that *ceacam1L*-overexpressing hGICs formed larger tumors than parental hGICs at 40 days after injection and induced massive hemorrhages in tumors (Fig. 2E), consistent with the previous finding in which Ceacam1 acted as an angiogenesis-inducing extracellular factor (19). We further found that the tumors formed by *ceacam1L*-overexpressing hGICs contained more Ki67+ proliferating cells but less activated-Caspase 3+ dying cells than control tumors (Fig. 2F and 2G). These results indicated that Ceacam1L regulated GIC tumorigenesis intracellularly and tumor angiogenesis extracellularly.

Ceacam1L regulated the expression of stemness-related genes and the side population through STAT3 activation in GICs

In order to identify the molecular mechanism regulated by Ceacam1L, we compared the gene expression profile of *ceacam1L*-overexpressing NSCs with that of NSCs, in which the endogenous expression of *ceacam1L* was undetectable, and found that 1,347 genes were upregulated while 1,286 were downregulated in *ceacam1L*-overexpressing NSCs (Fig. S3A). Of these, we noted that the overexpression of *ceacam1L* strongly induced the expression of STAT3 target genes, including glial fibrillary acidic protein (GFAP), suppressor of cytokine signaling 3 (SOCS3), S100β, angiopoietin 1 (ANGPT1), and angiotensinogen (AGT), in NSCs (Fig. 3A). We confirmed that the overexpression of Ceacam1L induced the nuclear translocation of the phosphorylated form of STAT3

(p-STAT3) and GFAP expression in NSCs (Fig. 3B-D). These results indicated that Ceacam1L activated the STAT3 signaling pathway in NSCs.

We also compared the gene expression profile of NSCL61 with that of *ceacam1sh*-overexpressing NSCL61, and found that 4,864 genes were upregulated while 3,984 were downregulated in *ceacam1sh*-overexpressing NSCL61 (Figure S3A). We noted a significant down-regulation in the expression of stemness-related genes, including Notch factors (*notch3*, *notch4*, *hey1*, and *dll1*), aldehyde dehydrogenases (ALDHs) (*aldh-1a1*, *-1a3*, *-1a7*, *-1l1*, *-1l2*, and *-3b1*), SRY-box transcription factors (*sox-1*, *-2*, *-3*, *-4*, and *-9*), ATP-Binding Cassette (ABC) transporters (*abc-a1*, *-a3*, *-a7*, *-b8*, *-c3*, *-c5*, *-c10*, *-d1*, and *-g4*), *angpt1*, *epidermal growth factor receptor (egfr)*, *chemokine receptor 4 (cxcr4)*, *patched 1*, and *stat3* in *ceacam1sh*-overexpressing NSCL61 (Fig. S3B). Since STAT3 is a well-known important factor for both stemness and tumorigenesis (20-23), we determined which genes were potential Ceacam1L/STAT3 targets using the Champion ChiP Transcription Factor Search Portal based on the SABiosciences' proprietary database (http://www.sabiosciences.com/chipqpcrsearch.php), and found that *dll1*, *hey1*, *notch* (*3* and *4*), *sox* (*1*, *2*, and *9*), *abc* (*a1*, *b8*, and *c5*), *angpt1*, *egfr*, *cxcr4*, *patched 1*, and *stat3*, contained the putative STAT3 binding sites (Fig. S3B). We confirmed that the overexpression of *dnSTAT3* as well as that of *ceacam1sh* decreased the expression of *sox1*, *aldh1a1*, *cxcr4*, *dll1*, *notch3*, and *hey1* in hGICs (Fig. 4A and B). We verified that the overexpression of *dnSTAT3* inhibited GFAP expression in E3 cells, even when cultured in differentiation medium with 10% FCS (Fig. 4C), and E3 proliferation in NSC medium (Fig. 4D).

We then examined whether Ceacam1L was indeed involved in the stemness maintenance in GICs. We found that the overexpression of Ceacam1L strongly increased the SP (9.0% -> 30%) (Fig. 5A), whereas that of *ceacam1sh* abolished the population in hGICs (9.3% -> 1.2%) (Fig. 5B). The overexpression of Ceacam1L up-regulated the expression of GFAP in NSC medium and that of Nestin in 1% FCS medium, whereas the knockdown of Ceacam1 down-regulated the expression of Nestin in NSC medium (Fig. 5C). The expression level of neuronal (Tuj1) and oligodendrocyte (GC) markers did not change by either Ceacam1L overexpression or knockdown. We verified that *ceacam1L*-overexpressing hGICs kept the neurosphere formation activity even when cultured sparsely, whereas the parental hGICs lost their self-renewal activity in the same condition (Fig. S4). Furthermore, we found that *ceacam1L*-overexpression made hGICs to be resistant to the temozolomide (TMZ), which is a standard anti-GBM medicine (Fig. S5): although the blood concentration of TMZ is 50-200μM for GBM patients, the *ceacam1L*-overexpressing hGICs survived even in the presence of 1mM TMZ. Together with data that Aldh1a11, one of Ceacam1L-downstream factors, mediated TMZ resistance (24), these findings suggested that Ceacam1L confers TMZ resistance in GICs through the induced expression of Aldh1a1.

The monomeric Ceacam1L cytoplasmic tail activated c-Src-dependent STAT3 signaling, whereas its oligomerization abolished this activity

Ceacam1L was previously shown to activate the signaling factor, c-Src and two protein tyrosine phosphatases, non-receptor type 6 and 11 (PTPN6 and 11, also known as SHP-1

and -2, respectively), upon phosphorylation of the Ceacam1L-cytoplasmic tail by various types of tyrosine kinase receptors (10,11,25). In turn, c-Src and PTPN6 then activated and inactivated STAT3 respectively, while PTPN11 modulated the Ras, NF-κB, and EGFR signaling pathways positively and the JAK/STAT pathway negatively (26-29). We found that hGICs expressed *ptpn11* and *c-Src*, but not *ptpn6* (Fig. 6A) and that the phosphorylated forms of PTPN11 (p-PTPN11) and c-Src (p-c-Src) bound to Ceacam1L in hGICs (Fig. 6B), indicating that the Ceacam1L-dependent negative feedback signal, which blocks STAT3 activation, was abolished in hGICs.

We evaluated whether c-Src activated STAT3 in hGICs. The overexpression of a constitutive active form of c-Src (caSrc) not only increased STAT3 phosphorylation and GFAP expression, but also enhanced cell proliferation, whereas the overexpression of a dominant negative form of c-Src (dnSrc) inhibited these inductions (Fig. 6C and D). These results suggested that Ceacam1L regulated GIC proliferation through the activation of c-Src/STAT3 signaling.

Ceacam1L exists as a monomer, cis-/trans-homodimer, or cis-/trans-heterodimer with Ceacam1 splicing variants or other Ceacam family members; therefore, the intracellular domain of Ceacam1L is a monomer or homodimer, depending on the circumstances (10,11). To determine which form of the Ceacam1L cytoplasmic tail activated c-Src/STAT3 signaling, we constructed two chimera proteins, FGC1L and FGC1S, consisting of FLAG, a part of the extracellular domain of the granulocyte colony-stimulating factor receptor, the Ceacam1-transmembrane domain, and either the cytoplasmic tail of Ceacam1L or Ceacam1S, respectively (Fig. 7A). We established

FGC1L- and FGC1S-expressing hGIC and NSC lines, cultured them in the presence or absence of an anti-FLAG antibody, and then examined the phosphorylation of c-Src and STAT3 as well as the expression of GFAP. We found that p-c-Src, p-STAT3, and GFAP levels were increased in FGC1L-expressing hGICs in the absence of the antibody, whereas these inductions were not detected in FGC1L-expressing hGICs treated with the antibody or FGC1S-expressing cells (Fig. 7B). We confirmed these results using FGC1L- and FGC1S-expressing NSC lines (Fig. 7C). We demonstrated that FGC1L associated with p-c-Src and p-PTPN11 in hGICs in the absence of the antibody (Aggregation–), whereas these associations were abolished in antibody-treated FGC1L-expressing cells (Fig. 7D). We also confirmed these results using FGC1L-expressing NSC lines (Fig. 7E). Thus, these results revealed that the monomeric Ceacam1L cytoplasmic tail activated c-Src/STAT3 signaling in GICs (Fig. 7A).

Discussion

Ceacam1 is known to be involved in various biological functions, including proliferation, angiogenesis, tumorigenesis, and inhibition of both cytokine production by and cytotoxic activity of immune cells, as an intracellular and intercellular factor (19,30). We showed that Ceacam1L-overexpressing hGICs formed larger colonies in soft agar and tumors with massive hemorrhaging in the brains of immunodeficient mice, whereas the knockdown of Ceacam1 blocked GIC proliferation. In addition to previous findings in which Ceacam1 acted as a major effector of vascular endothelial growth factor-induced angiogenesis (19,31), we revealed that Ceacam1L regulated the expression of Angpt1, interleukin 18, and secretogranin II, all of which play an important role in vascular development and angiogenesis in GICs (32-34). Since neovascularization is not only a common characteristic of GBM, but has also been correlated with poor outcomes, these findings indicate that Ceacam1L is an indispensable therapeutic target for GBM.

Ceacam1L is a highly glycosylated protein that carries a Lewis X (LeX) structure, also known as CD15 and SSEA1 (35,36), which is a well-known stem cell marker expressed on many types of normal stem cells, including embryonic stem cells, bone marrow stem cells, neural stem cells (37-39), and GICs (18). We herein confirmed that over 90% of $CD15^{high}$ GICs were positive for Ceacam1 when GICs were immunolabeled in the presence of TritonX-100, suggesting that CD15-carrying Ceacam1 mainly existed in the cytoplasm. This may also explain why CD15-negative glioma cells self-renewed and formed tumorspheres similar to CD15-positive glioma cells (40). Since Ceacam1L was previously shown to be expressed at low levels on the surface of resting T cells and was

quickly mobilized from the intracellular compartment to the cell surface following T cell activation (41), the molecular mechanisms regulating Ceacam1L mobilization in GICs need to be elucidated in more detail.

We found that Ceacam1L positively regulated the expression of a number of stemness-related genes in GICs both directly and indirectly. Ceacam1L controlled the expression of NSC factors (dll1, notch3, hey1, and Sox1-4, 9) and astrocyte markers (GFAP and S100β) in GICs, suggesting that Ceacam1L+ GICs may retain the characteristics of radial glial cells or subventricular astrocytes, both of which behave as multipotential NSCs in the adult brain (42,43). We also found that *ceacam1L*-overexpression kept self-renewal capability in hGICs. Since Ceacam1L regulated the expression of many ABC transporters and ALDH family members in GICs, Ceacam1L appears to widely govern drug resistance in GICs. Indeed, we found that the *ceacam1L*-overexpressing hGICs were much more resistant to TMZ, the standard medicine for GBM, than the parental hGICs. This is consistent with a finding that Aldh1a1, one of down stream factors of Ceacam1L, mediated TMZ resistance in GBM, although the detail mechanism remained elusive (25). Furthermore, FGC1L-overexpressing NSCs formed larger spheres in cultures and continued to express Nestin even in differentiation medium with 1% FCS. These results suggest that Ceacam1L contributed to the maintenance of stemness in GICs. It is unlikely that STAT3, a crucial Ceacam1L signaling factor, predominated the expression of all Ceacam1L-downstream genes; therefore, the transcription factor, other than STAT3, that controls the expression of stemness-related genes needs to be identified.

When phosphorylated by EGFR, Ceacam1L was shown to activate c-Src, PTPN6, and PTPN11 and also enhance or prevent the proliferation signals of the receptor in a cell type-dependent manner (11,44,45). We unexpectedly found that the expression of PTPN6, which prevents the Janus kinase (JAK)-dependent STAT3 signaling pathway (46), was silenced in hGICs, suggesting that a Ceacam1L-dependent negative feedback signal to EGFR was abolished in hGICs. Taken together with the finding that PTPN11 and c-Src activated EGFR and STAT3 signals, respectively (21,27, this manuscript), our results suggest that Ceacam1L acted as an amplifier of both EGFR and STAT3 signaling in hGICs.

We demonstrated that the monomeric Ceacam1L-cytoplasmic tail activated c-Src/STAT3 signaling, whereas its oligomerization abolished this activity. The state of Ceacam1L (monomer or oligomer) in GICs may be dependent on their circumstances, in which GIC-associating (niche) cells, such as immune cells and microglia, may express Ceacam1L-binding partners, including Ceacam1L, 1S, soluble forms of Ceacam1 and Ceacam5 (10-12). The finding that lung metastasis by Ceacam1+ B16F10 melanoma cells was significantly decreased in Ceacam1-knockout mice revealed that the expression of Ceacam1 on tumor-associating cells was essential for successful tumorigenesis (47). In fact, we found the association of Ceacam1+/EGFR+ cells and CD68+ activated microglia in human GBM tissues (Supplementary Fig. 6). It has been shown that CD68+ cells increased in high-grade gliomas (48) and that CD68+ infiltrating microglias/macrophages were involved in gliomagenesis (49). Together, these suggest that CD68+ microglias/macrophages play a crucial part to maintain/activate GICs in the niche. Therefore, next crucial challenge is

to investigate how Ceacam1L-dependent intercellular association between GICs and their surrounding cells regulates GIC maintenance and tumor-niche formation.

Disclosure of Potential Conflicts of Interest

No potential conflicts of interest were disclosed

Author Contributions

Conception and design: T. Kondo

Development of methodology: T. Kondo

Acquisition of data: S. Kaneko, Y, Nakatani, T. Takezaki, T. Hide, D. Yamashita, N. Ohtsu, S. Terasaka, T. Kondo

Analysis and interpretation of data: S. Kaneko, Y, Nakatani, T. Takezaki, T. Hide, D. Yamashita, N. Ohtsu, T. Kondo

Writing, and review: T. Kondo

Study supervision: T. Kondo, T. Ohnishi, K. Houkin

Grant Support

This work was supported, in part, by a research program of the Project for Development of Innovative Research on Cancer Therapeutics (P-DIRECT), Ministry of Education, Culture, Sports, Science and Technology of Japan, to T.K.

Acknowledgments

We thank Shigekazu Nagata for mouse GCSFR cDNA, Shizuo Akira for the mouse dominant-negative form of STAT3 (dnSTAT3) cDNA, Chitose Oneyama for the c-Src-expression vectors (caSrc and dnSrc), and Yoshihiro Tsukamoto for a TMZ assay.

References

1. Singh SK, Clarke ID, Terasaki M, Bonn VE, Hawkins C, Squire J, et al. Identification of a cancer stem cell in human brain tumors. Cancer Res 2003;63:5821-8.
2. Singh SK, Clarke ID, Hide T, Dirks PB. Cancer stem cells in nervous system tumors. Oncogene 2004;23:7267-73.
3. Kondo T. Brain cancer stem-like cells. Eur J Cancer 2006;42:1237-42.
4. Vescovi AL, Galli R, Reynolds BA. Brain tumour stem cells. Nat Rev Cancer 2006;6:425-36.
5. Alvarez-Buylla A, Lois C. Neuronal stem cells in the brain of adult vertebrates. Stem Cells 1995;13:263-72.
6. Frisén J, Johansson CB, Lothian C, Lendahl U. Central nervous system stem cells in the embryo and adult. Cell Mol Life Sci 1998;54:935-45.
7. Hide T, Takezaki T, Nakatani Y, Nakamura H, Kuratsu J, Kondo T. Sox11 prevents tumorigenesis of glioma-initiating cells by inducing neuronal differentiation. Cancer Res 2009;69:7953-9.
8. Hide T, Takezaki T, Nakatani Y, Nakamura H, Kuratsu J, Kondo T. Combination of a Ptgs2 inhibitor and an EGFR signaling inhibitor prevents tumorigenesis of oligodendrocyte lineage derived glioma-initiating cells. Stem Cells 2011;29:590-9.
9. Yamashita D, Kondo T, Ohue S, Takahashi H, Ishikawa M, Matoba R, et al. miR-340 acts as a tumor suppressor in tumorigenesis of human glioma-initiating cells by targeting plasminogen activator, tissue. Cancer Res In press.

10. Gray-Owen SD, Blumberg RS. CEACAM1: contact-dependent control of immunity. Nat Rev Immunol 2006;6:433-46.
11. Kuespert K, Pils S, Hauck CR. CEACAMs: their role in physiology and pathology. Curr Opin Cell Biol 2006;18:565-71.
12. Nagaishi T, Iijima H, Nakajima A, Chen D, Blumberg RS. Role of CEACAM as a regulator of T cells. Ann NY Acad Sci 2006;1072:155-75.
13. Fuller GN, Bigner SH. Amplified cellular oncogenes in neoplasms of the human central nervous system. Mutat. Res 1992;276:299-306.
14. Kondo T, Raff M. Chromatin remodeling and histone modification in the conversion of oligodendrocyte precursors to neural stem cells. Genes Dev 2004;18:2963-72.
15. Kondo T, Setoguchi T, Taga T. Persistence of a small subpopulation of cancer stem-like cells in the C6 glioma cell line. Proc Natl Acad Sci USA 2004;101:781-6.
16. Thomas M, Klibanov AM. Enhancing polyethylenimine's delivery of plasmid DNA into mammalian cells. Proc Natl Acad Sci USA 2002;99:14640-5.
17. Takanaga H, Tsuchida-Straeten N, Nishide K, Watanabe A, Aburatani H, Kondo T. Gli2 is a novel regulator of sox2 expression in telencephalic neuroepithelial cells. Stem Cells 2009;27:165-74.
18. Son MJ, Woolard K, Nam DH, Lee J, Fine HA. SSEA-1 is an enrichment marker for tumor-initiating cells in human glioblastoma. Cell Stem Cell 2009;4:440-52.
19. Ergün S, Kilik N, Ziegeler G, Hansen A, Nollau P, Götze J, et al. CEA-related cell adhesion molecule 1: a potent angiogenic factor and a major effector of vascular endothelial growth factor. Mol Cell 2000;5:311-20.

20. Bromberg JF, Wrzeszczynska MH, Devgan G, Zhao Y, Pestell RG, Albanese C, et al. Stat3 as an oncogene. Cell 1999;98:295-303.
21. Silva CM. Role of STATs as downstream signal transducers in Src family kinase-mediated tumorigenesis. Oncogene 2004;23:8017-23.
22. Liu Y, Li C, Lin J. STAT3 as a Therapeutic Target for Glioblastoma. Anticancer Agents Med Chem 2010;10:512-9.
23. Carpenter RL, Lo HW. STAT3 Target Genes Relevant to Human Cancers. Cancers 2014;6:897-925.
24. SchäferA, Teufel J, Ringel F, Bettstetter M, Hoepner I, Rasper M, et al. Aldehyde dehydrogenase 1A1-a new mediator of resistance to temozolomide in glioblastoma. Neuro Oncol 2012;14:1452-64.
25. Müller MM, Klaile E, Vorontsova O, Singer BB, Obrink B. Homophilic adhesion and CEACAM1-S regulate dimerization of CEACAM1-L and recruitment of SHP-2 and c-Src. J Cell Biol 2009;187:569-81.
26. Qu CK, Yu WM, Azzarelli B, Feng GS. Genetic evidence that Shp-2 tyrosine phosphatase is a signal enhancer of the epidermal growth factor receptor in mammals. Proc Natl Acad Sci USA 1999;96:8528-33.
27. You M, Yu DH, Feng GS. Shp-2 tyrosine phosphatase functions as a negative regulator of the interferon-stimulated Jak/STAT pathway. Mol Cell Biol 1999;19:2416-24.
28. You M, Flick LM, Yu D, Feng GS. Modulation of the nuclear factor kappa B pathway by Shp-2 tyrosine phosphatase in mediating the induction of interleukin (IL)-6 by IL-1 or tumor necrosis factor. J Exp Med 2001;193:101-10.

29. Chong ZZ, Maiese K. The Src homology 2 domain tyrosine phosphatases SHP-1 and SHP-2: diversified control of cell growth, inflammation, and injury. Histol Histopathol 2007;22:1251-67.

30. Markel G, Lieberman N, Katz G, Arnon TI, Lotem M, Drize O, et al. CD66a interactions between human melanoma and NK cells: a novel class I MHC-independent inhibitory mechanism of cytotoxicity. J Immunol 2002;168:2803-10.

31. Horst AK, Ito WD, Dabelstein J, Schumacher U, Sander H, Turbide C, et al. Carcinoembryonic antigen-related cell adhesion molecule 1 modulates vascular remodeling in vitro and in vivo. J Clin Invest 2006;116:1596-605.

32. Park CC, Morel JC, Amin MA, Connors MA, Harlow LA, Koch AE. Evidence of IL-18 as a novel angiogenic mediator. J Immunol 2001;167:1644-53.

33. Metheny-Barlow LJ, Li LY. The enigmatic role of angiopoietin-1 in tumor angiogenesis. Cell Res 2003;13:309-17.

34. Fischer-Colbrie R, Kirchmair R, Kähler CM, Wiedermann CJ, Saria A. Secretoneurin: a new player in angiogenesis and chemotaxis linking nerves, blood vessels and the immune system. Curr Protein Pept Sci 2005;6:373-85.

35. Lucka L, Fernando M, Grunow D, Kannicht C, Horst AK, Nollau P, et al. Identification of Lewis x structures of the cell adhesion molecule CEACAM1 from human granulocytes. Glycobiology 2005;15:87-100.

36. Bogoevska V, Horst A, Klampe B, Lucka L, Wagener C, Nollau P. CEACAM1, an adhesion molecule of human granulocytes, is fucosylated by fucosyltransferase IX and

interacts with DC-SIGN of dendritic cells via Lewis x residues. Glycobiology 2006;16:197-209.

37. Solter D, Knowles BB. Monoclonal antibody defining a stage-specific mouse embryonic antigen (SSEA-1). Proc Natl Acad Sci USA 1978;75:5565-9.
38. Fox N, Damjanov I, Martinez-Hernandez A, Knowles BB, Solter D. Immunohistochemical localization of the early embryonic antigen (SSEA-1) in postimplantation mouse embryos and fetal and adult tissues. Dev Biol 1981;83:391-8.
39. Capela A, Temple S. LeX/ssea-1 is expressed by adult mouse CNS stem cells, identifying them as nonependymal. Neuron 2002;35:865-75.
40. Patru C, Romao L, Varlet P, Coulombel L, Raponi E, Cadusseau J, et al. CD133, CD15/SSEA-1, CD34 or side populations do not resume tumor-initiating properties of long-term cultured cancer stem cells from human malignant glio-neuronal tumors. BMC Cancer 2010;10:66.
41. Nakajima A, Iijima H, Neurath MF, Nagaishi T, Nieuwenhuis EE, Raychowdhury R, et al. Activation-induced expression of carcinoembryonic antigen-cell adhesion molecule 1 regulates mouse T lymphocyte function. J Immunol 2002;168:1028-35.
42. Doetsch F, Caillé I, Lim DA, García-Verdugo JM, Alvarez-Buylla A. Subventricular zone astrocytes are neural stem cells in the adult mammalian brain. Cell 1999;97:703-16.
43. Chojnacki AK, Mak GK, Weiss S. Identity crisis for adult periventricular neural stem cells: subventricular zone astrocytes, ependymal cells or both? Nat Rev Neurosci 2009;10:153-63.

44. Poy MN, Ruch RJ, Fernstrom MA, Okabayashi Y, Najjar SM. Shc and CEACAM1 interact to regulate the mitogenic action of insulin. J Biol Chem 2002;277:1076-84.

45. Abou-Rjaily GA, Lee SJ, May D, Al-Share QY, Deangelis AM, Ruch RJ, et al. CEACAM1 modulates epidermal growth factor receptor--mediated cell proliferation. J Clin Invest 2004;114:944-52.

46. Bousquet C, Susini C, Melmed S. Inhibitory roles for SHP-1 and SOCS-3 following pituitary proopiomelanocortin induction by leukemia inhibitory factor. J Clin Invest 1999;104:1277-85.

47. Arabzadeh A, Chan C, Nouvion AL, Breton V, Benlolo S, DeMarte L, et al. Host-related carcinoembryonic antigen cell adhesion molecule 1 promotes metastasis of colorectal cancer. Oncogene 2013;32:849-60.

48. Prosniak M, Harshyne LA, Andrews DW, Kenyon LC, Bedelbaeva K, Apanasovich TV, et al. Glioma grade is associated with the accumulation and activity of cells bearing M2 monocyte markers. Clin Cancer Res 2013;19:3776-86.

49. Garofalo S, D'Alessandro G, Chece G, Brau F, Maggi L, Rosa A, et al. Enriched environment reduces glioma growth through immune and non-immune mechanisms in mice. Nat Commun 2015;6:6623.

Figure Legends

Figure 1. Ceacam1 was predominantly expressed in GICs

(A) *Ceacam1* expression in mNSCs, NSCL61, mOPCs, OPCL61, hNSC, and hGICs, E3 and E6, examined by RT-PCR. The expression of *gapdh* was used as an internal control. (B) Representative data of NSCL61, OPCL61, and hGICs immunostained for Ceacam1 (green). (C) Representative images of immunoreactivity for Ceacam1 (green) and CD15 (red) in one of three primary human GBM specimens (D) Representative images of immunoreactivity for Ceacam1 (green) and EGFR (red) in one of three primary human GBM specimens. (E) Representative data from an expression analysis of Ceacam1 and CD15 in one of three human GBMs by flow cytometry. Nuclei were counterstained with DAPI (blue). Scale bar: 100 μm.

Figure 2. Ceacam1L was involved in GIC malignant phenotypes

(A) The decreased proliferation of *ceacam1sh*-expressing NSCL61, OPCL61, and hGICs, E3 and E6. (B) The colony formation ability of *ceacam1sh*-expressing NSCL61, OPCL61, and hGICs in soft agar was lower than that of *controlsh* (*contsh*)-expressing cells. (C) The colony formation ability of *ceacam1L*-overexpressing hGICs (ceacam1L) in soft agar was greater than that of control hGICs (cont). (D) Survival curves for mice injected with cont (black dotted line) or ceacam1L (red solid line). Data are displayed as the mean±SEM with n=5 mice per group. (E) Representative images of H&E staining of tumors formed by cont and ceacam1L at 40 days after transplantation. White dotted area indicate tumor. Left panels show the high magnification images of black dashed squares. (F) Increased

proliferation of *ceacam1L*-overexpressing hGICs, compared with their parental cells. (G) Decreased number of the activated-Caspase 3 (Casp3)-positive cells in *ceacam1L*-overexpressing hGICs, compared with their parental cells. Scale bar: 0.5 mm.

Figure 3. Ceacam1L overexpression activated STAT3 signaling in NSCs

(A) Microarray data of STAT3-target genes that were significantly up-regulated in NSCs by the overexpression of Ceacam1L. (B) Control NSCs (cont) and Ceacam1L-overexpressing NSCs (ceacam1L) were immunostained for phosphorylated STAT3 (p-STAT3, green) and Ceacam1 (red). (C) Cont and ceacam1L were immunostained for GFAP (green) and Ceacam1 (red). (D) The enforced expression of *ceacam1L* increased p-STAT3 and GFAP in NSCs. Scale bar: 50 μm, 20 μm (insets).

Figure 4. The dominant negative form of STAT3 decreased the expression of stemness-related genes and GFAP in hGICs and inhibited GIC proliferation

(A, B) RT-PCR analysis of the expression of *sox1*, *aldh1a1*, *cxcr4*, *dll1*, *notch3*, and *hey1* in *ceacam1sh*- (A) and *dnSTAT3*- (B) overexpressing E3 cells. The expression of *gapdh* was used as an internal control. (C) dnSTAT3-expressing E3 cells (arrows, green) were negative for GFAP (red), even when cultured in the differentiation medium. Nuclei were counterstained with DAPI (blue). Scale bar: 20 μm. (D) Overexpression of dnSTAT3 inhibited the proliferation of E3 cells. * $p<0.01$.

Figure 5. Ceacam1L levels affected SP and Nestin expression in hGICs

(A) Representative data of SP in control E3 and *ceacam1L*-overexpressing cells. The SP, which disappeared in the presence of 10 μM reserpine (right panels), is outlined and shown as a percentage of the total cell population. (B) Representative data of SP in control E3 and *ceacam1sh*-overexpressing cells, as in (A). (C) Ratio of the neural differentiation marker-positive control, *ceacam1L*- and *ceacam1sh*-overexpressing E3 cells, when cultured under the indicated conditions. * $p<0.05$, ** $p<0.01$.

Figure 6. Activated c-Src bound to Ceacam1L and induced STAT3 phosphorylation and cell proliferation (A) RT-PCR analysis of the expression of *c-Src*, *ptpn6*, and *ptpn11* in hGICs and hNSC. The expression of *gapdh* was used as an internal control. (B) A binding analysis of the phosphorylated forms of both c-Src and PTPN11 with Ceacam1L in E3 cells (left panel). Cell lysates were analyzed for these factors by western blotting (right panel). (C) Influence of GFAP expression and phosphorylation of STAT3 and c-Src by overexpression of the constitutive-active form of c-Src (caSrc) and the dominant-negative form of c-Src (dnSrc) in E3 cells. (D) Effects of the overexpression of caSrc and dnSrc on the proliferation of E3 cells. * $p<0.01$, ** $p<0.001$.

Figure 7. The Ceacam1L monomer activated c-Src/STAT3 signaling (A) A model of FGC1L monomer-dependent activation of the c-Src/STAT3 signaling pathway. (B, C) A western blotting analysis of c-Src/STAT3 phosphorylation and GFAP expression in FGC1S- and FGC1L-expressing hGICs (B) and mNSCs (C) in the presence (+) or absence (-) of a FLAG antibody. (D, E) A binding analysis of the phosphorylated forms of both c-Src and

PTPN11 with FGC1L in hGICs (D) and mNSCs (E), in the presence (aggregation +) and absence (aggregation –) of a FLAG antibody (left panel). Cell lysates were analyzed for these factors by western blotting (right panels).

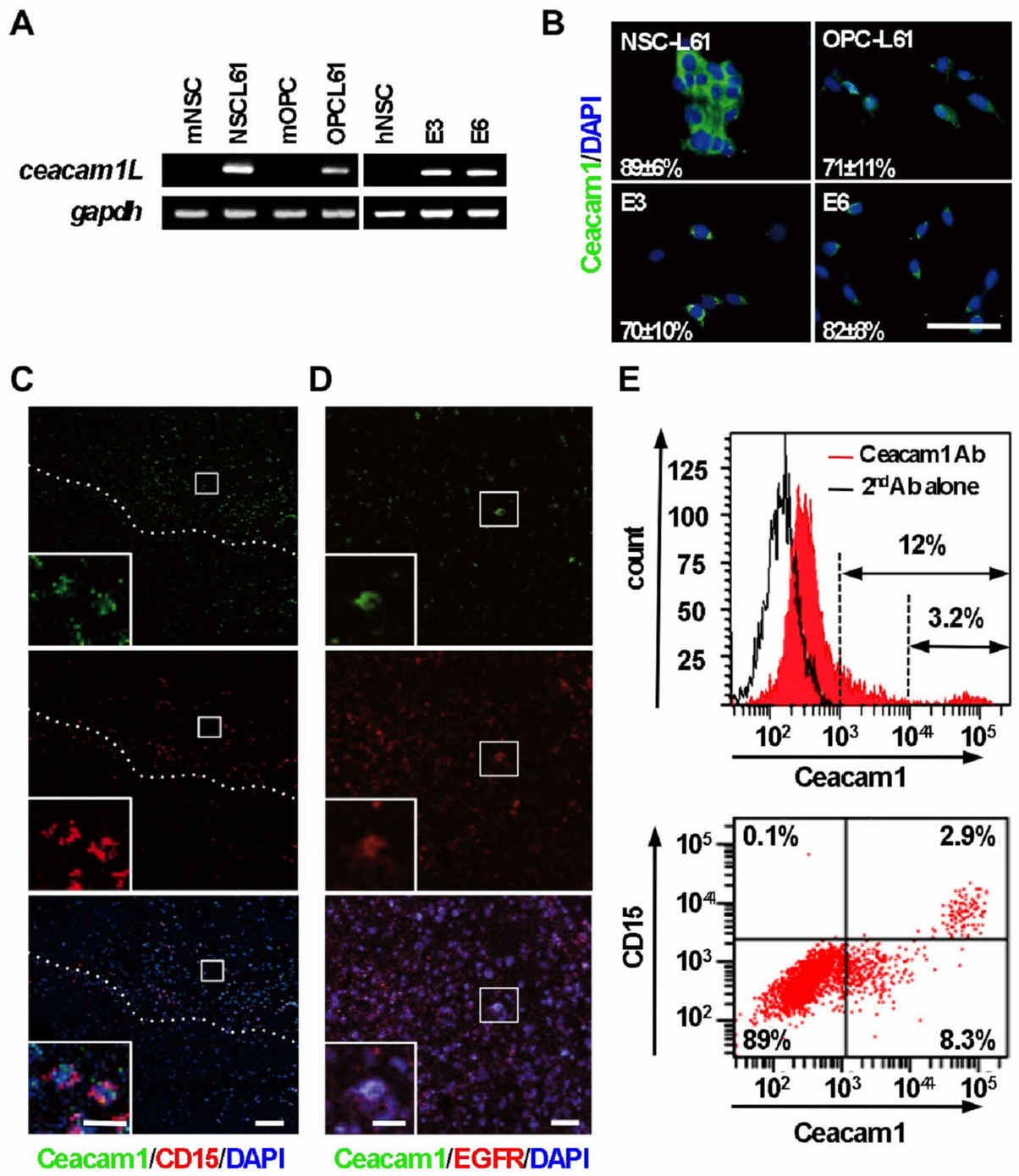
A
mNSC
NSCL61
mOPC
OPCL61
hNSC
E3
E6
ceacam1L
gapdh
B
NSC-L61
OPC-L61
E3
E6
Ceacam1/DAPI
89±6%
71±11%
70±10%
82±8%
C
D
E
Ceacam1/CD15/DAPI
Ceacam1/EGFR/DAPI
Ceacam1 Ab
2nd Ab alone
count
125
100
75
50
25
12%
3.2%
10^2
10^3
10^4
10^5
Ceacam1
CD15
0.1%
2.9%
89%
8.3%

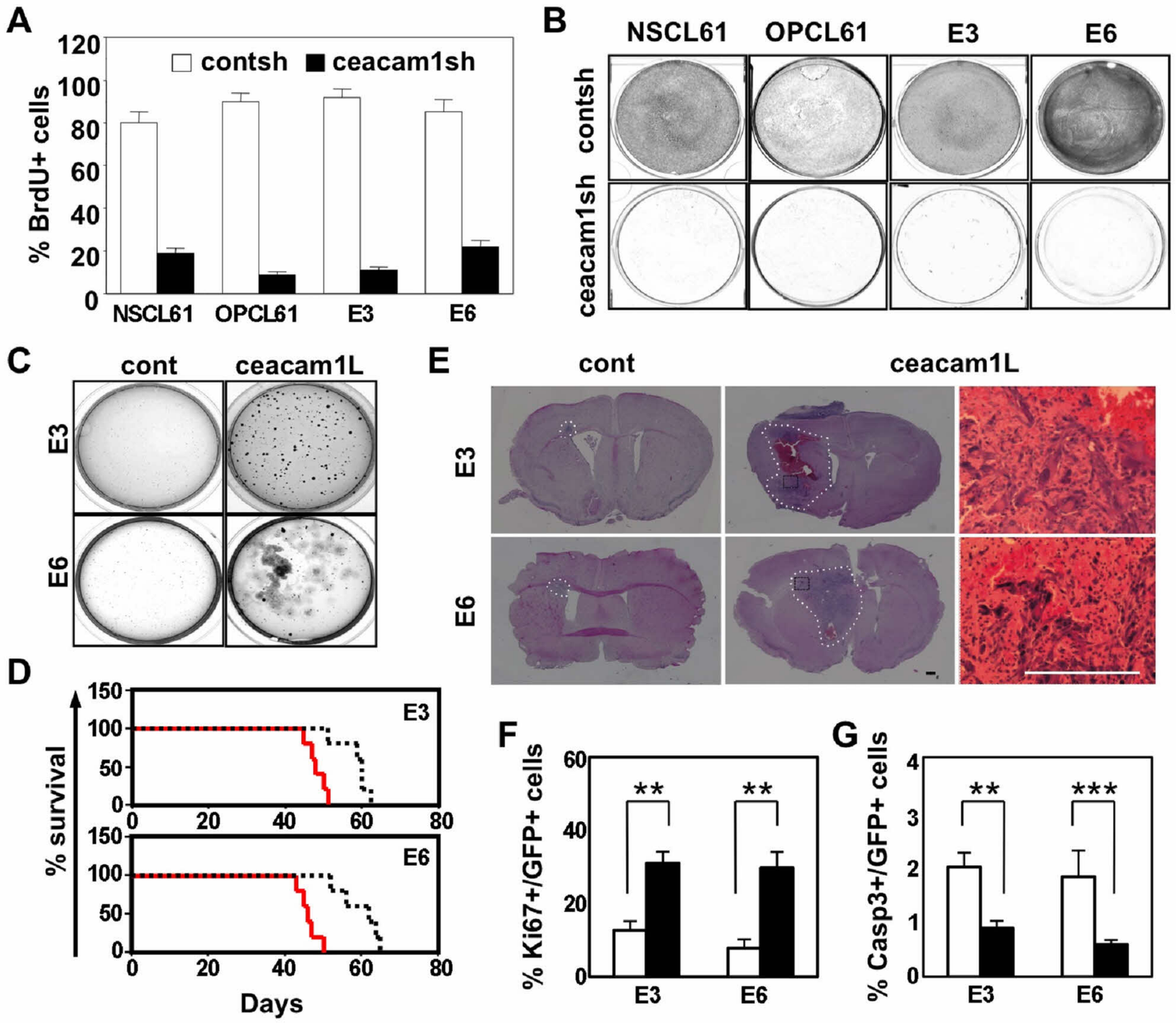
A
contsh
ceacam1sh
% BrdU+ cells
120
100
80
60
40
20
0
NSCL61
OPCL61
E3
E6
B
NSCL61
OPCL61
E3
E6
contsh
ceacam1sh
C
cont
ceacam1L
E3
E6
D
% survival
150
100
50
0
E3
E6
0
20
40
60
80
Days
E
cont
ceacam1L
E3
E6
F
% Ki67+/GFP+ cells
60
40
20
0
**
**
E3
E6
G
% Casp3+/GFP+ cells
4
3
2
1
0
**
***
E3
E6

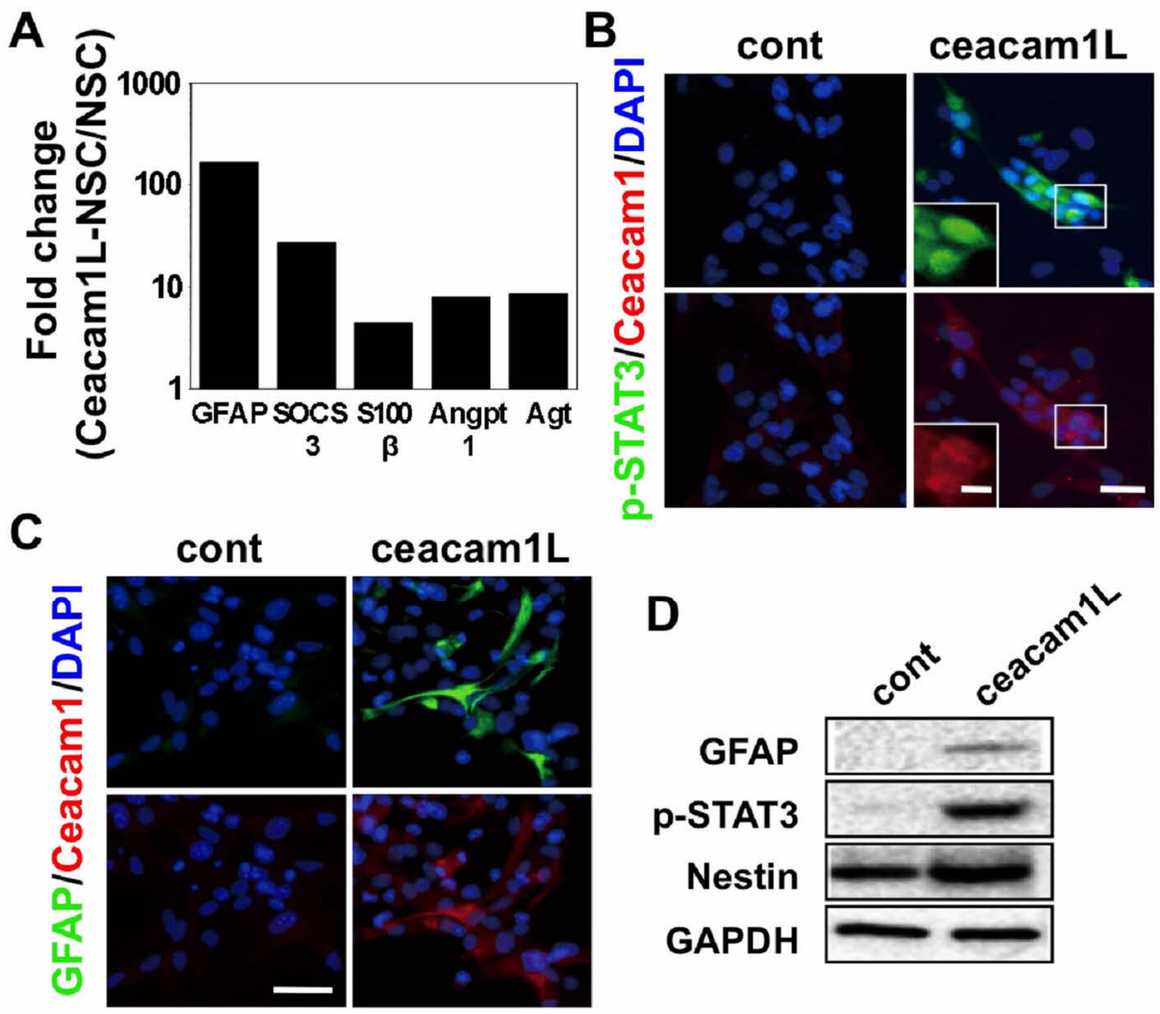
A
Fold change
(Ceacam1L-NSC/NSC)
1000
100
10
1
GFAP
SOCS 3
S100 β
Angpt 1
Agt
B
cont
ceacam1L
p-STAT3/Ceacam1/DAPI
C
cont
ceacam1L
GFAP/Ceacam1/DAPI
D
cont
ceacam1L
GFAP
p-STAT3
Nestin
GAPDH

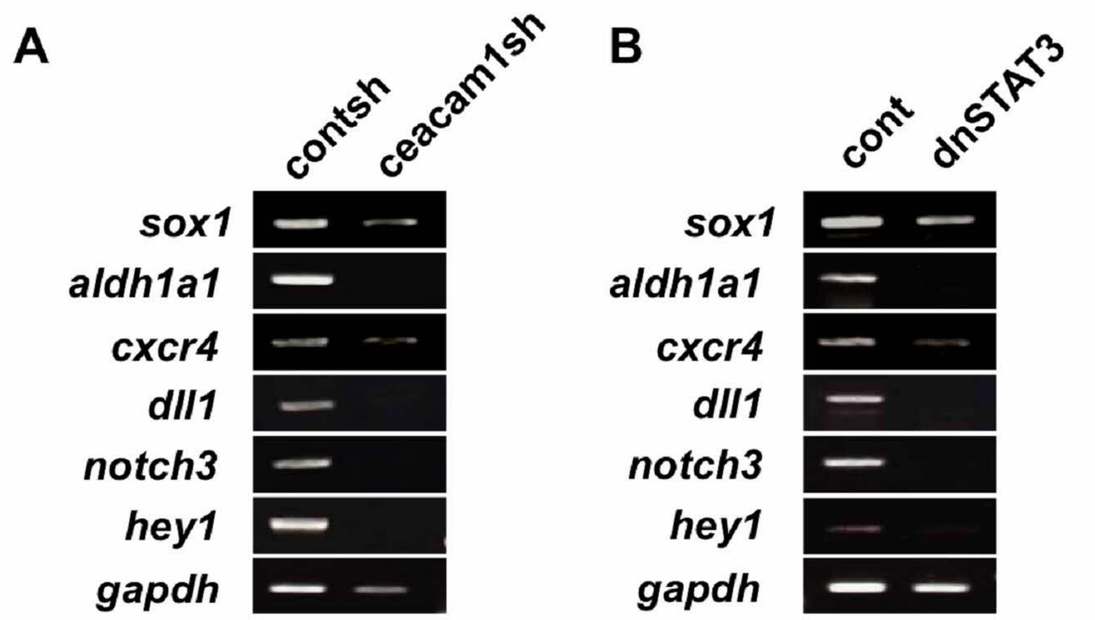
A
contsh
ceacam1sh
sox1
aldh1a1
cxcr4
dll1
notch3
hey1
gapdh
B
cont
dnSTAT3
sox1
aldh1a1
cxcr4
dll1
notch3
hey1
gapdh
C
GFP/GFAP/DAPI
D
% BrdU+ cells
100
80
60
40
20
0
*
cont
dnSTAT3

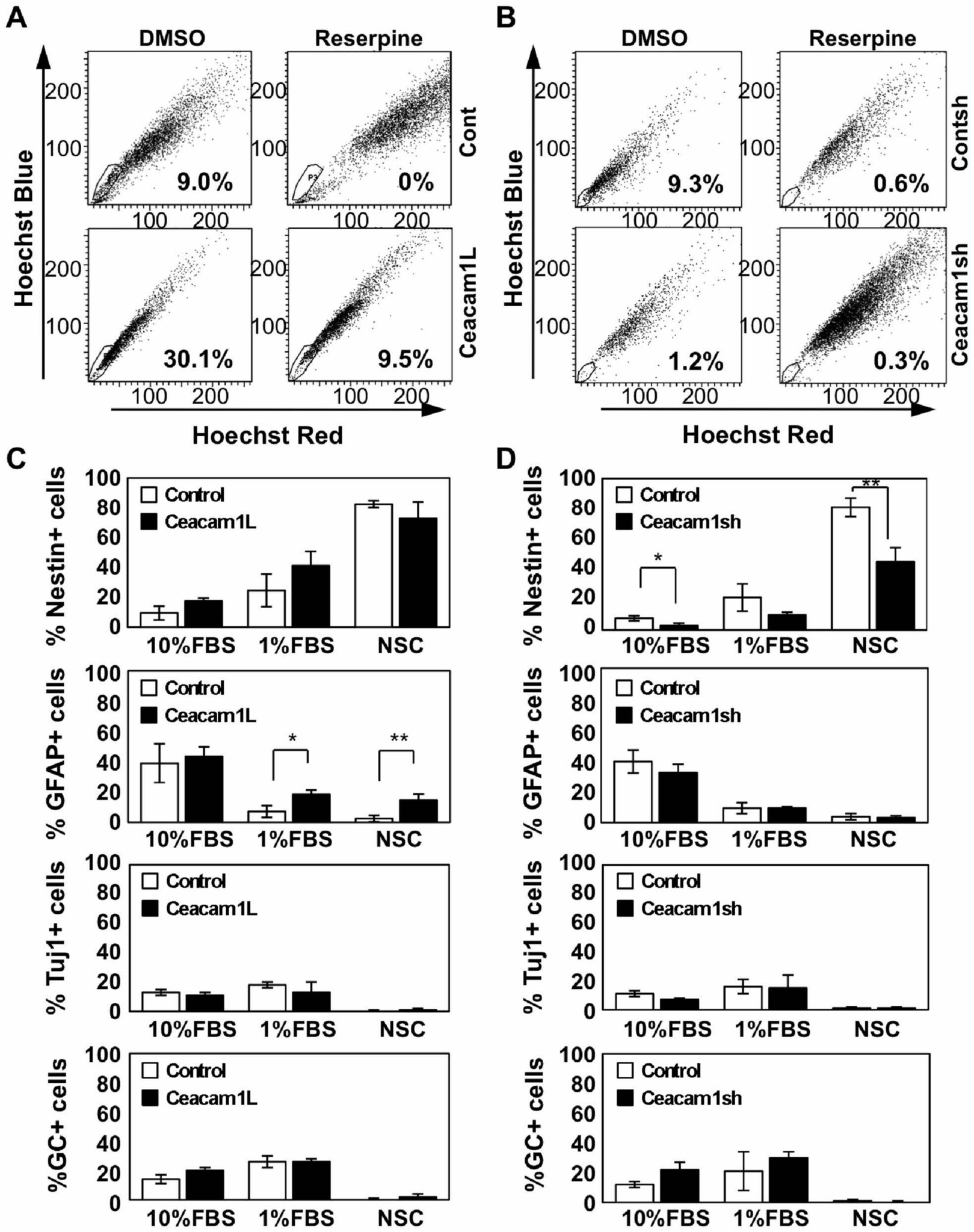
A
DMSO
Reserpine
Hoechst Blue
Hoechst Red
Cont
Ceacam1L
9.0%
0%
30.1%
9.5%
B
DMSO
Reserpine
Contsh
Ceacam1sh
9.3%
0.6%
1.2%
0.3%
C
D
% Nestin+ cells
% GFAP+ cells
% Tuj1+ cells
%GC+ cells
Control
Ceacam1L
Ceacam1sh
10%FBS
1%FBS
NSC
*
**

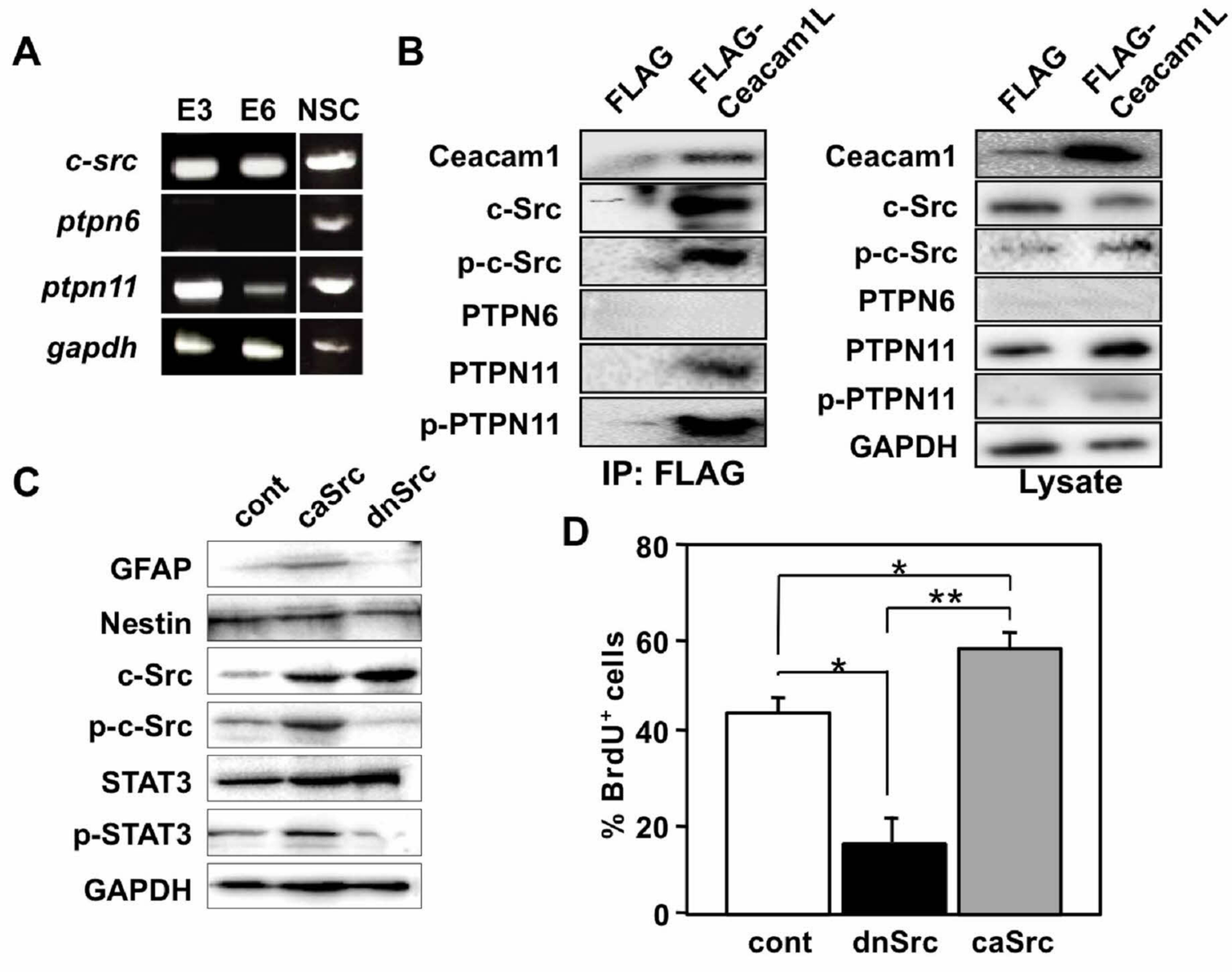
A
E3
E6
NSC
c-src
ptpn6
ptpn11
gapdh
B
FLAG
FLAG-Ceacam1L
Ceacam1
c-Src
p-c-Src
PTPN6
PTPN11
p-PTPN11
IP: FLAG
Ceacam1
c-Src
p-c-Src
PTPN6
PTPN11
p-PTPN11
GAPDH
Lysate
C
cont
caSrc
dnSrc
GFAP
Nestin
c-Src
p-c-Src
STAT3
p-STAT3
GAPDH
D
% BrdU+ cells
80
60
40
20
0
*
**
*
cont
dnSrc
caSrc

Kaneko, et al, Figure 7

A

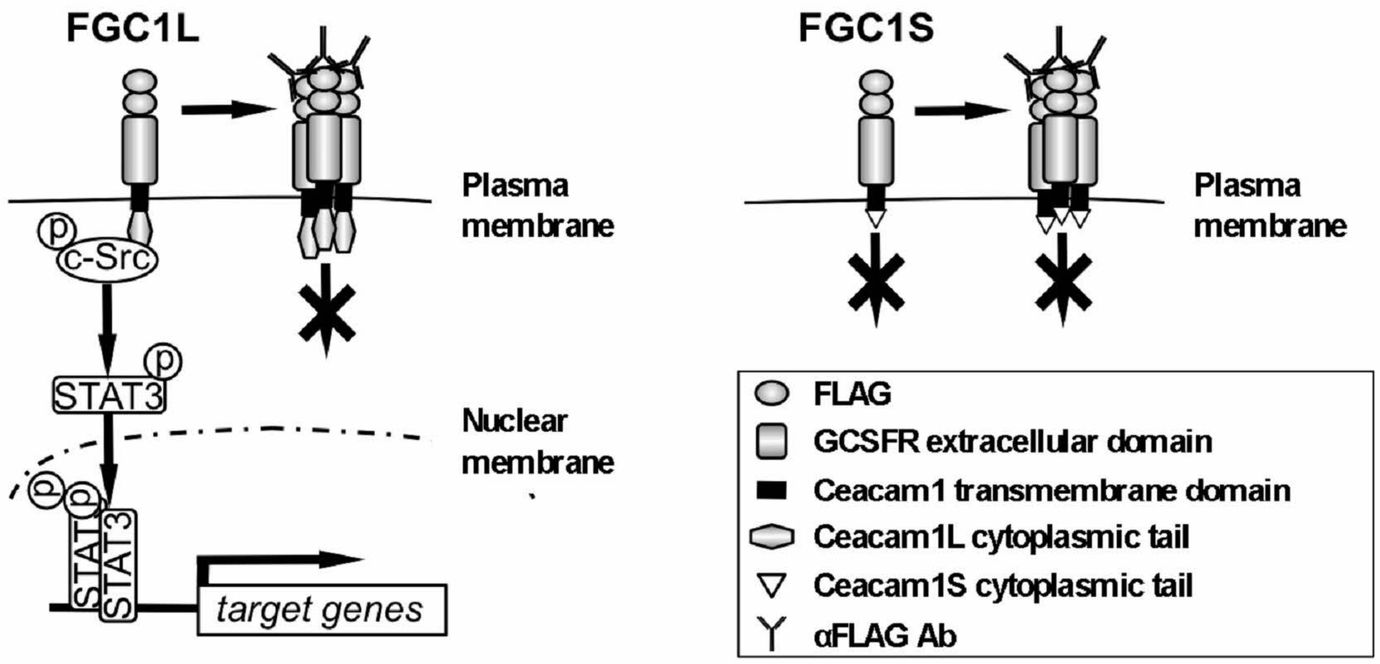

B

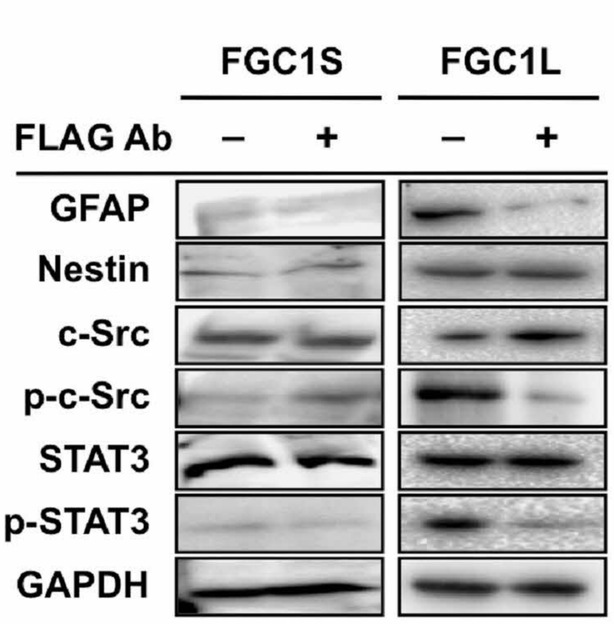

C

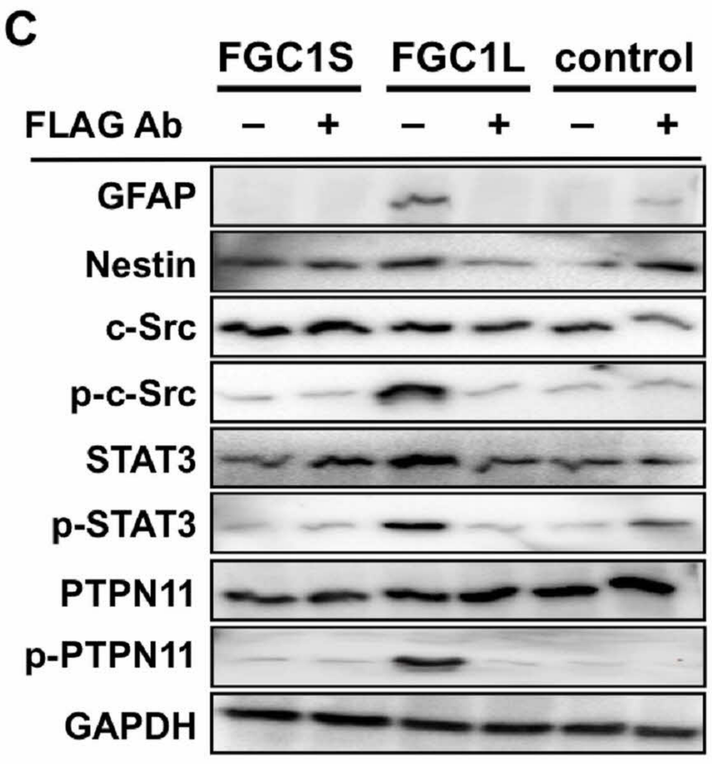

D

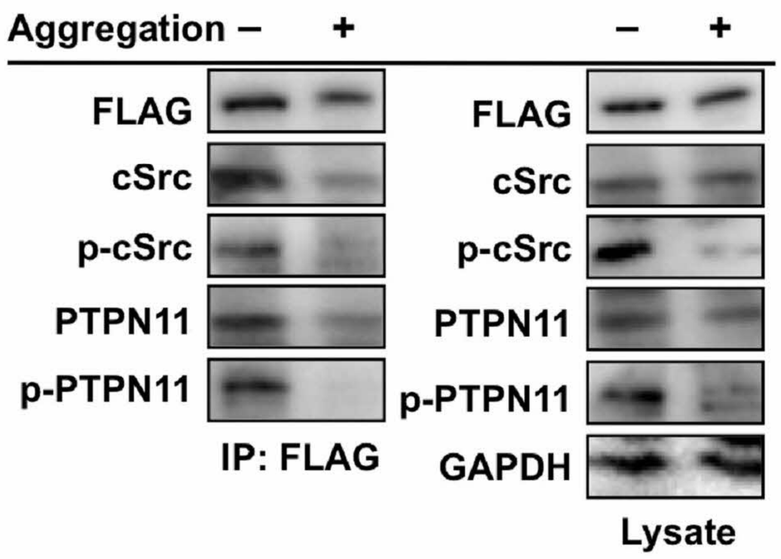

E